The EMBO Journal (2010) 29, 4210–4222 | © 2010 European Molecular Biology Organization | All Rights Reserved 0261-4189/10
www.embojournal.org

THE EMBO JOURNAL

RNAi-based screening identifies the Mms22L–Nfkbil2 complex as a novel regulator of DNA replication in human cells

Wojciech Piwko[1,4,*], Michael H Olma[1,4], Michael Held[1], Julien N Bianco[2], Patrick GA Pedrioli[1,5], Kay Hofmann[3], Philippe Pasero[2], Daniel W Gerlich[1] and Matthias Peter[1,*]

[1]Institute of Biochemistry, Department of Biology, ETH Zurich, Zurich, Switzerland, [2]Institute of Human Genetics, CNRS UPR 1142, Montpellier, France and [3]Miltenyi Biotec GmbH, Bioinformatics Department, Bergisch-Gladbach, Germany

Cullin 4 (Cul4)-based ubiquitin ligases emerged as critical regulators of DNA replication and repair. Over 50 Cul4-specific adaptors (DNA damage-binding 1 (Ddb1)–Cul4-associated factors; DCAFs) have been identified and are thought to assemble functionally distinct Cul4 complexes. Using a live-cell imaging-based RNAi screen, we analysed the function of DCAFs and Cul4-linked proteins, and identified specific subsets required for progression through G1 and S phase. We discovered *C6orf167*/Mms22-like protein (*Mms22L*) as a putative human orthologue of budding yeast Mms22, which, together with cullin Rtt101, regulates genome stability by promoting DNA replication through natural pause sites and damaged templates. Loss of Mms22L function in human cells results in S phase-dependent genomic instability characterised by spontaneous double-strand breaks and DNA damage checkpoint activation. Unlike yeast Mms22, human Mms22L does not stably bind to Cul4, but is degraded in a Cul4-dependent manner and upon replication stress. Mms22L physically and functionally interacts with the scaffold-like protein Nfkbil2 that co-purifies with histones, several chromatin remodelling and DNA replication/repair factors. Together, our results strongly suggest that the Mms22L–Nfkbil2 complex contributes to genome stability by regulating the chromatin state at stalled replication forks.
The EMBO Journal (2010) **29,** 4210–4222. doi:10.1038/emboj.2010.304; Published online 26 November 2010
Subject Categories: proteins; genome stability & dynamics
Keywords: cell division; DNA damage repair; DNA replication

*Corresponding authors: W Piwko or M Peter, Institute of Biochemistry, Department of Biology, ETH Zurich, 8093 Zurich, Switzerland.
Tel.: +41 44 63 32 564; Fax: +41 44 63 21 298;
E-mail: wojciech.piwko@bc.biol.ethz.ch or
Tel.: +41 44 63 36 586; Fax: +41 44 63 21 298;
E-mail: matthias.peter@bc.biol.ethz.ch
[4]These authors contributed equally to this work
[5]Present address: The Scottish Institute for Cell Signalling, The Sir James Black Centre, College of Life Sciences, University of Dundee, Dow Street, Dundee DD1 5EH, Scotland

Received: 20 September 2010; accepted: 5 November 2010; published online: 26 November 2010

Introduction

Accurate and complete DNA duplication is fundamental to the maintenance of genomic integrity and is ensured by the cooperation of cell cycle checkpoints and DNA repair pathways. However, progressing replication forks encounter many obstacles, including tightly packed histone-associated heterochromatic regions, a myriad of non-nucleosomal protein impediments such as sites of active transcription, telomeres and centromeres, and damaged templates (Tourriere and Pasero, 2007). Dedicated mechanisms are required to slow down and modify active replication forks at these sites and require checkpoint-dependent stabilisation of the replisome. Occasionally, however, replication forks collapse and must be rescued by the firing of late origins or by specialised restart/repair processes that prevent the formation of double-strand breaks (DSBs), illegitimate recombination and gross chromosomal rearrangements. Although these mechanisms are of crucial importance to maintain genome integrity, little is known about the components and regulatory signals.

The phosphatidylinositol 3 kinase-related protein kinases (PIKKs), ATM, ATR and DNA-dependent protein kinase (DNA-PK), emerged as key factors in several DNA damage response pathways. ATM and DNA-PK are activated primarily by the presence of DSBs, whereas stalled replication forks and the presence of replication protein A (RPA)-coated ssDNA stimulate ATR (Shiloh, 2003; Cimprich and Cortez, 2008). ATM and ATR and their major effector kinases Chk2 and Chk1 slow down or arrest cell cycle progression to allow time for efficient repair. In addition, PIKKs orchestrate DNA damage repair in a manner not only specific for the type of damage but also for the cell cycle stage at which the lesion occurs. DSBs, one of the most toxic DNA lesions, are repaired by two major mechanisms—non-homologous end joining (NHEJ) and homologous recombination (HR). NHEJ leads to ligation of two DNA ends without sequence homology and is predominantly used to repair breaks occurring during G1 or in specialised cases during S phase. In contrast, HR occurs preferentially in S and G2 and takes advantage of the presence of the sister chromatid, which is used as a template for error-free homology-driven repair (Branzei and Foiani, 2008).

In addition to phosphorylation, DNA replication and repair pathways are regulated at multiple levels by ubiquitylation of key components, in particular by cullin 4 (Cul4)-RING E3 ubiquitin ligases (CRL4) (Lee and Zhou, 2007). All cullins interact via their C-terminal region with the RING finger protein Rbx1/Hrt1, which in turn recruits an E2 ubiquitin-conjugating enzyme. The N-terminal domain of cullins is specific for each subfamily, and interacts with distinct classes of substrate-specific adaptors (Pintard *et al*, 2004). The human genome encodes two Cul4-paralogues, Cul4A and

Cul4B, both of which bind via their N-terminal regions to the DNA damage-binding 1 (Ddb1) protein. In turn, Ddb1 interacts with the various substrate-specific adaptor subunits, which belong to a large group of WD40 repeat (WDR)-containing proteins (Ddb1–Cul4-associated factors; DCAFs). However, the critical substrates and specific DCAFs involved in DNA replication and repair processes remain poorly understood.

$CRL4^{Cdt2}$ regulates several S phase-related processes by using the replicative polymerase sliding clamp PCNA as a cofactor to target the replication-licensing factor Cdt1 (Kim and Kipreos, 2007), the cyclin-dependent kinase (CDK) inhibitor p21 (Abbas *et al*, 2008) and the TLS polymerase eta Polη (Kim and Michael, 2008). Moreover, Cul4 complexes control two nucleotide excision repair (NER) pathways. For example, $CRL4^{Ddb2}$ is recruited to UV-induced DNA lesions, where it mediates ubiquitylation of the repair protein XPC (Sugasawa *et al*, 2005), while the $CRL4^{CSA}$ complex targets CSB for degradation to remove stalled RNA polymerase II from damaged templates (Sugasawa *et al*, 2005; Fousteri *et al*, 2006). CRL4 complexes also support efficient DNA repair by altering nucleosome stability around the damaged site. For example, Cul4 ubiquitylates histone H2A, H3 and H4 near UV lesions, thereby causing histone eviction to expose the damaged DNA to repair proteins (Kapetanaki *et al*, 2006; Wang *et al*, 2006).

Progression of DNA replication in Cul4-depleted cells is perturbed and accompanied by strong upregulation of the phosphorylated histone H2A variant H2AX (γH2AX), indicating the occurrence of spontaneous DSBs during the S phase (Olma *et al*, 2009). This is reminiscent of the function of Rtt101, the putative Cul4 orthologue in budding yeast, which, in complex with Mms1 and Mms22, has a crucial role in DNA replication through natural pause sites and damaged templates (Luke *et al*, 2006). Indeed, detailed studies revealed that *rtt101*Δ cells are genetically unstable because they are unable to promote HR at stalled replication forks during S phase (Duro *et al*, 2008). Mms22 binds to the N-terminal region of Rtt101 via Mms1, which shares significant similarities to human Ddb1, suggesting that Mms22 is a substrate-specific adaptor for the Rtt101-based ubiquitin ligase (Zaidi *et al*, 2008). Finally, genetic and biochemical experiments suggest that the $Rtt101^{Mms22}$ E3 ligase functions downstream of Rtt109, a histone acetyltransferase required for H3-K56 acetylation, which marks newly replicated DNA and is required for genome stability maintenance in yeast and mammalian cells (Collins *et al*, 2007; Roberts *et al*, 2008). These studies suggest that a conserved Rtt101/Cul4-dependent pathway may be involved in replicating through chromosomal slow zones and promotes restart of stalled replication forks.

In this study, we used automated live-cell microscopy and computational image analysis to quantify interphase timing in an RNAi screen, targeting all known and bioinformatically predicted substrate adaptors of Cul4. We identified several Cul4-associated proteins specifically regulating the duration of the G1, S and G2 phases of the cell cycle, and C6orf167/Mms22-like protein (Mms22L), a putative human homologue of yeast Mms22. Biochemical and cell biological analysis suggests that Mms22L, in complex with Nfkbil2, is required to ensure genome stability during DNA replication in mammalian cells.

Results

RNAi-based screening for Cul4-linked genes involved in cell cycle progression

To investigate the functional importance of the different Cul4 substrate adaptors for DNA replication and genome integrity, we developed an automated RNAi-based screening protocol allowing quantification of replication and mitosis timing. We used a HeLa cell line stably expressing mCherry-tagged histone H2B as a chromatin marker to discriminate the mitotic stages, and EGFP-tagged PCNA to visualise the characteristic morphological changes of DNA replication foci during the S phase (Figure 1A). Automated time-lapse imaging data were annotated using the CellCognition computational framework (Held *et al*, 2010) to classify 11 different cell cycle stages by supervised machine learning (G1, early, mid and late S, and G2 phase based on EGFP-PCNA, and six mitotic stages based on H2B-mCherry; Figure 1A and B), which allowed to measure the duration of each single cell cycle stage. To validate the sensitivity and performance of this assay, we analysed the phenotype of HeLa cells that were RNAi-depleted for the known cell cycle regulators Skp2, Ddb1 and Rad51 (Figure 1C). In agreement with previous publications, downregulation of each of these genes resulted in the expected delays in G1, S and G2 phases, respectively (Sonoda *et al*, 1998; Sutterluty *et al*, 1999; Lovejoy *et al*, 2006).

To identify Cul4 adaptors involved in DNA replication, we designed an siRNA library targeting 147 genes associated with Cul4, including known and bioinformatically predicted DCAFs and other Cul4-interacting proteins (Figure 2A and Supplementary Table 1). Each gene was targeted by three to six distinct siRNA oligos (Supplementary Table 1), using reverse transfection in 96-well plates. Image acquisition was started 25 h after RNAi and cells were imaged for 47 h with a time resolution of approximately 6 min. Using the CellCognition software, we measured the duration of the respective cell cycle phases for at least 15 cells per siRNA, and used the calculated medians to classify each of the candidate genes. If more than half of all quantified siRNAs showed a *z*-score above 5, relative to the negative controls, we considered this gene as a potential hit. In all, 50 genes showed a significant delay in G1 phase (Supplementary Table 2), including 17 *bona fide* DCAFs characterised by WD40 domains (Figure 2B). As an example, Figure 2C and D illustrate the analysis of cells depleted of DCAF Wdr51B, which extended G1 phase to approximately 15 h, compared with 7 h for RNAi controls. Four DCAFs were not only necessary for timely G1 progression but also exhibited significant delays in S phase. Among them is the known DCAF, Wdr26, which slows down DNA replication by approximately 20%, as visualised by persistent PCNA foci (Supplementary Table 2, Figure 2E and F). In addition, we identified seven genes including four DCAFs specifically required for efficient progression through S phase, without significantly affecting G1 and G2 length. Taken together, this RNAi-based screen identified a subset of known or predicted CRL4 adaptors required for timely interphase progression, and suggested specific functions of CRL4-based E3 ligases in G1, entry into S phase and efficient progression through early and late stages of DNA replication.

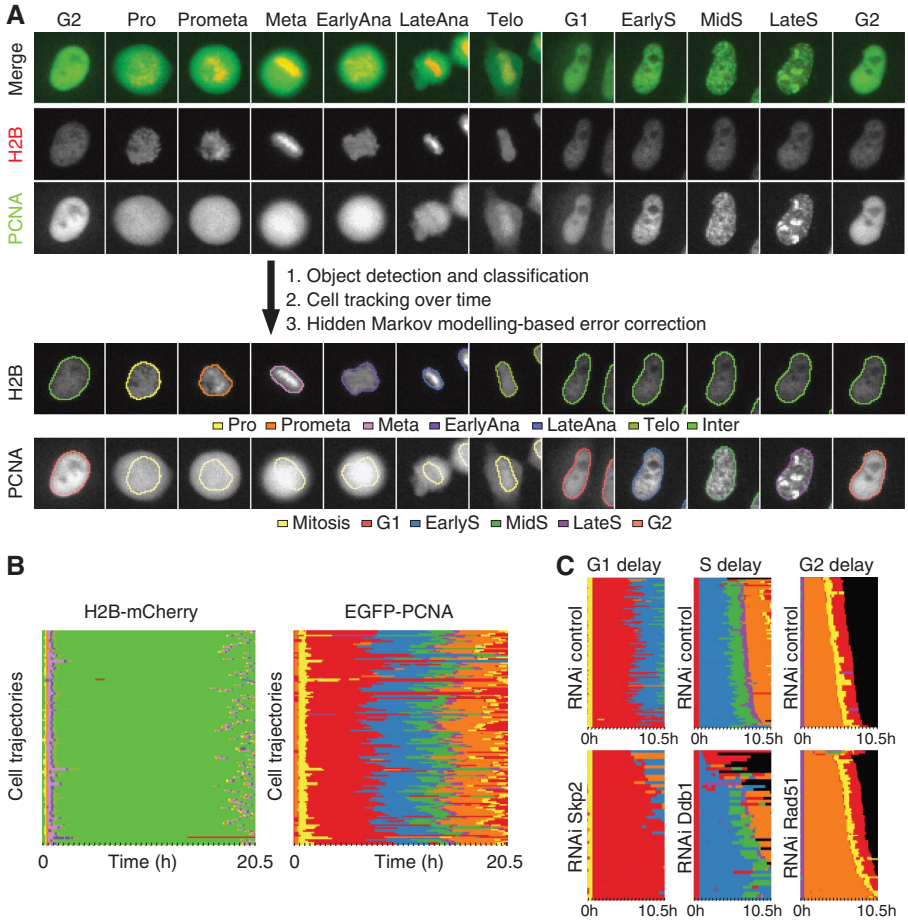

Figure 1 Automated high-content RNAi screening assay to measure the timing of different cell cycle phases. (**A**) HeLa cells stably expressing the chromatin marker H2B-mCherry (red) and the replication factory marker EGFP-PCNA (green) were imaged for 47 h using an automated wide-field epifluorescence microscope with a 10 × dry objective. Single cells were detected by local adaptive thresholding and distinct cellular morphologies were classified by supervised machine learning. Trajectories of single cells containing prometaphase stages were extracted and classification was improved with a hidden Markov model (HMM)-based method (Held *et al*, 2010). This yielded accurate annotations of all indicated cell cycle phases (lower panels) and apoptosis (not shown). (**B**) Overview of all detected cell trajectories for an RNAi control in the two channels sorted by occurrence in the movie and aligned at the prophase–prometaphase transition. (**C**) Cell trajectories detected in time-lapse movies of cells RNAi-depleted of Skp2, Ddb1 and Rad51 (oligos 11, 7 and 6), aligned at the mitosis-G1, G1-early S phase and late S phase–G2 transitions and sorted by G1, S and G2 phase length, respectively.

C6orf167/Mms22L is required for maintenance of genomic stability during S phase

Downregulation of only two genes, *PolR2E* and *C6orf167*, caused a significant prolongation of G2 phase. The pronounced G2 delay of C6orf167-depleted cells classified with an average *z*-score of 20 and, in contrast to PolR2E, was not accompanied by changes in G1 or S phase duration (Figure 2G and H; Supplementary Table 3). Interestingly, *C6orf167* codes for a yet uncharacterised human protein with low, but significant, similarity to yeast Mms22 (Supplementary Figure 1). Given the bioinformatic conservation and functional similarities in maintaining genome stability during DNA replication, we named *C6orf167* as Mms22L.

To test whether the prolonged G2 phase in Mms22L-depleted cells results from activation of the DNA damage checkpoint, we performed immunoblot analysis of extracts derived from HeLa cells treated with siRNA specifically targeting Mms22L, using phospho-specific antibodies against activated checkpoint proteins. Indeed, we observed increased phosphorylation of ATM on Ser 1981, Chk2 on Thr 68 and Chk1 on Ser 345 upon depletion of Mms22L (Figure 3A and Supplementary Figure 2), which suggests activation of both the ATM and ATR branches of the DNA damage checkpoint. This was accompanied by hyperphosphorylation of several PIKK substrates, including the histone H2A variant H2AX on Ser 139 (γH2AX) and RPA2, markers of DNA damage and replication stress, respectively (Anantha *et al*, 2007). Similar results were also observed for U2OS cells (Supplementary Figure 3; Supplementary data not shown), implying that the defects are not solely explained by the transformed phenotype of HeLa cells. The G2 arrest may be a direct consequence of DNA damage checkpoint activation, as the G2 phase duration of Mms22L-depleted HeLa cells treated with the ATM/ATR inhibitor caffeine was reduced from 8.8 to 4.7 h, which is comparable to RNAi controls (Figure 3B). Taken together, these results suggest that depletion of Mms22L induces a strong delay in G2 because of activation of the ATM/ATR-dependent checkpoint response pathway.

To corroborate these results, we used indirect immunofluorescence microscopy using antibodies specific for γH2AX to visualise DSBs. Indeed, the number of γH2AX foci strongly

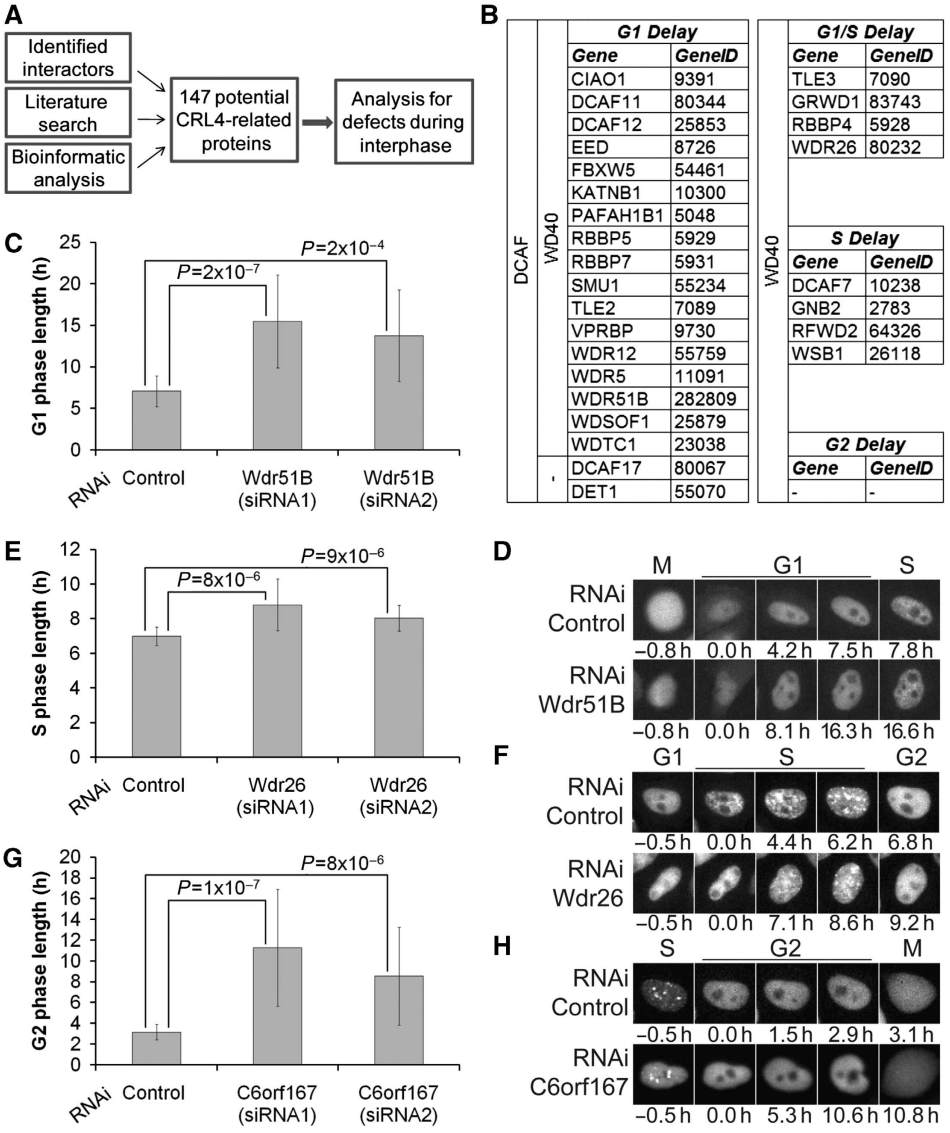

Figure 2 RNAi-based screen for Cul4-related genes involved in regulation of interphase in HeLa cells. (**A**, **B**) An RNAi library targeting Cul4-associated genes was based on MS analysis of purified Cul4A complexes and yeast two-hybrid screens of Cul4A and Cul4B. This list was complemented with published Cul4 interactors and detailed bioinformatic analysis of Cul4-related proteins. A total of 147 CRL4-related genes were then analysed by RNAi depletion for interphase delays using the automated screening assay depicted in Figure 1. *Bona fide* DCAFs showing specific delays at the indicated cell cycle phase are listed (**B**). The entire list including all analysed genes is provided in Supplementary Table 2. (**C**–**H**) The duration of the indicated cell cycle phase was measured for at least 20 cells depleted of selected candidates, and the mean, s.d. and the Student *t*-test *P*-value were calculated (**C**, **E**, **G**; oligos 2, 4, 5, 4, 7 and 8, respectively). Time-lapse microscopy images of a representative cell depleted for the indicated Cul4-related proteins, progressing through G1 (**D**, oligo 2), S (**F**, oligo 5) and G2 (**H**, oligo 7) phases.

increased upon RNAi depletion of Mms22L in HeLa (Figure 3C and D, and Supplementary Figure 2) and U2OS cells (Supplementary Figure 3). Moreover, this signal colocalised with foci formed by 53BP1 (Figure 3C), an important mediator of ATM signalling (Schultz *et al*, 2000; Wang *et al*, 2002), and RPA2 (Figure 3D), which marks extended ssDNA regions (Binz *et al*, 2004). We also examined Mms22L-depleted cells by flow cytometry (Figure 3E). As expected, the cell cycle analysis showed dramatic accumulation of cells in G2/M, and a concomitant reduction of cells in both G1 and S phase. Staining with γH2AX-specific antibodies revealed that DSBs gradually accumulate during S phase and partially diminish during G2 (Figure 3E and F). In contrast, γH2AX was only weakly increased during G1, suggesting that, in the absence of Mms22L, accumulation of DSBs arising specifically during S phase triggers a checkpoint-dependent arrest in G2 to allow sufficient time for repair before entering mitosis. Consistent with a specific function during the S phase, DNA combing experiments revealed that replication forks moved significantly slower in U2OS cells depleted for Mms22L in comparison with the RNAi control (Figure 3G and Supplementary Figure 4). Collectively, these phenotypes are reminiscent of yeast cells lacking components of the $Rtt101^{Mms22}$ E3 ligase, which regulates faithful DNA replication through damaged templates or replication slow zones (Duro *et al*, 2008; Zaidi *et al*, 2008). Because *rtt101*Δ and *mms22*Δ cells are strongly sensitive to genotoxic agents causing DNA damage during S phase (Luke *et al*, 2006; Collins *et al*,

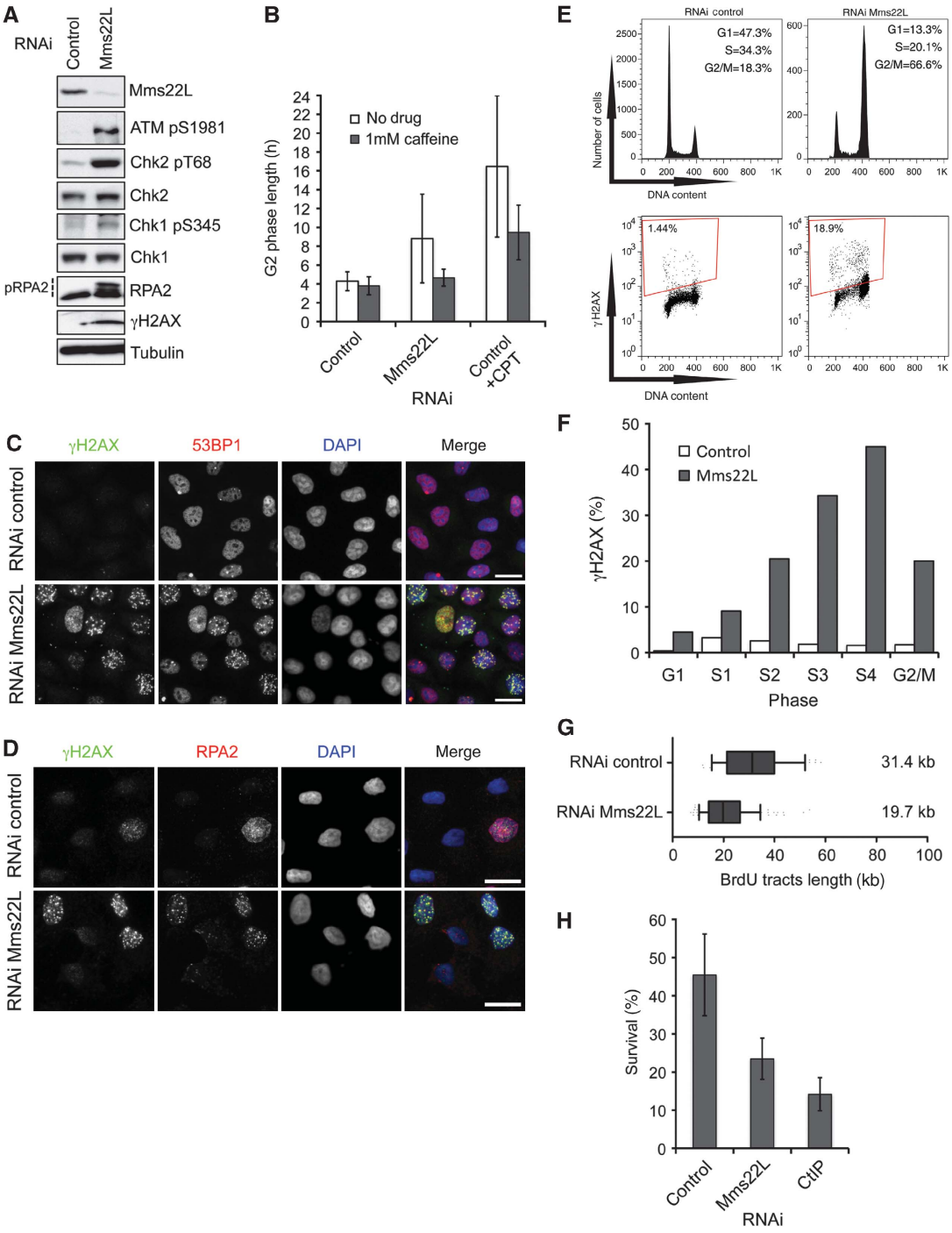

Figure 3 C6orf167/Mms22L is required to maintain genome integrity during the S phase. (**A**) Extracts from HeLa cells treated with control or Mms22L (oligo 1) siRNAs for 72 h were immunoblotted with specific antibodies recognising the indicated markers. pRPA2 marks phosphorylated forms of RPA2; tubulin was included as loading control. (**B**) Control and Mms22L-depleted (pooled oligos 1–3) HeLa cells expressing EGFP-PCNA and H2B-mCherry were imaged for 2 days with a time resolution of 26 min. Cells were either treated (grey bars) or not treated (white bars) with 1 mM caffeine to inhibit ATM/ATR. Where indicated, control cells were treated with 0.02 μM CPT to induce checkpoint activation (last column). G2 duration was determined from at least 25 cells for each condition based on the PCNA and H2B markers as described in Figure 1. (**C**, **D**) Mms22L-depleted (oligo 1) HeLa cells accumulate nuclear γH2AX foci that colocalise with 53BP1 (**C**) and RPA2 (**D**), as visualised by immunofluorescence analysis with specific antibodies. DNA was stained with DAPI; the scale bar represents 20 μm. (**E**, **F**) HeLa cells were treated with control and Mms22L (oligo 1) siRNAs for 72 h, and ethanol-fixed γH2AX-positive cells were quantified by flow cytometry using specific antibodies. Propidium iodide (PI) was used to stain DNA. The average percentage of γH2AX-positive cells is indicated in the gated area (**E**). S phase was divided into four subphases using FlowJo software, and the percentage of γH2AX-positive cells was measured for each cell cycle phase (**F**). (**G**) Single-molecule analysis of DNA replication in Mms22L-depleted U2OS cells. Cells treated with control or Mms22L (pooled oligos 1–3) siRNAs for 72 h were pulse-labelled for 20 min with BrdU. Fibres were stretched by DNA combing and labelled DNA was visualised by specific antibodies against BrdU. The graph shows the distribution and median values of BrdU tract length. Representative images of DNA fibres are shown in Supplementary Figure 4. (**H**) Mms22L downregulation causes CPT hypersensitivity. HeLa cells treated with control siRNA or siRNAs downregulating Mms22L (pooled oligos 1–3) were exposed for 1 h to 1 μM CPT, and the number of surviving colonies was determined after 8–10 days. Cells depleted for the HR-component CtIP were included for positive control. Bars with s.d. represent the percentage (%) of surviving colonies compared with untreated controls averaged from four independent experiments.

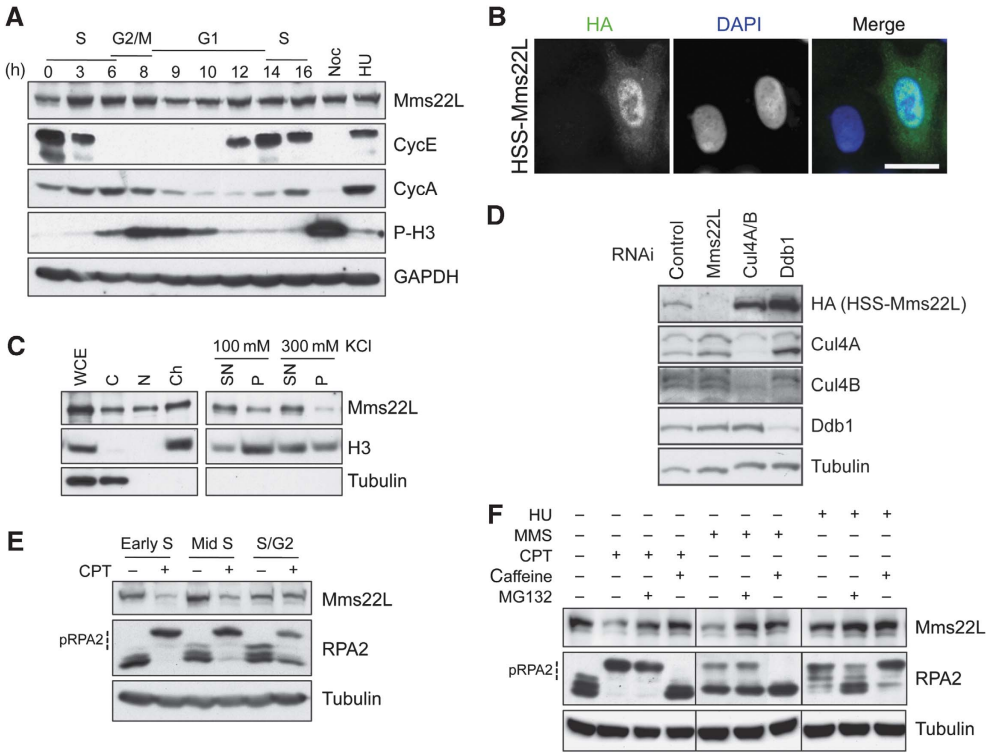

Figure 4 Mms22L levels are regulated throughout the cell cycle and upon DNA damage induced during S phase. (**A**) HeLa cells were synchronised in early S phase using the DTB/R protocol and harvested at the indicated time points after release from the second thymidine block (in hours). Nocodazole (Noc)- or HU-arrested cells were included as controls. Protein extracts were immunoblotted with antibodies against Mms22L and cell cycle markers cyclin E (S phase), cyclin A (S/G2) and phospho-Ser10 H3 (mitosis). GAPDH controls for equal loading. (**B**) The localisation of HSS-Mms22L was analysed after transient transfection by indirect immunofluorescence using anti-HA antibodies. DAPI visualises DNA; scale bar: 20 μm. (**C**) Mms22L is associated with chromatin. HeLa whole-cell extracts (WCE) were fractionated into cytosol (C), nucleoplasm (N) and chromatin (Ch) (left panels). The chromatin fraction was subjected to DNA digestion using micrococcal nuclease, incubated in buffer containing 100 or 300 mM KCl, and separated into soluble (SN) and pellet (P) fractions (right panels). Samples were analysed by immunoblotting with antibodies against Mms22L, the nuclear marker histone H3 and cytoplasmic tubulin. (**D**) HSS-Mms22L is stabilised in Cul4- and Ddb1-depleted cells. HeLa cells stably expressing HSS-Mms22L were RNAi-depleted of Mms22L (oligo 2), Cul4A and Cul4B or Ddb1 for 24 h. Doxycycline was added for an additional 24 h to induce HSS-Mms22L expression, and protein extracts were immunoblotted for the indicated proteins. (**E**, **F**) HeLa cells were synchronised by DTB/R and treated 2, 4 and 5.5 h after release with 1 μM CPT for 3 h. Mms22L levels were analysed by immunoblotting (**E**). HeLa cells synchronised in S phase (3 h after DTB/R) were treated with either 1 μM CPT, 0.05% (v/v) MMS, 2 mM HU, 20 μM MG132 or 5 mM caffeine, and analysed by immunoblotting with the indicated antibodies (**F**). Note that caffeine does not inhibit RPA2 phosphorylation induced by HU treatment, as demonstrated previously (Cortez, 2003).

2007; Zaidi *et al*, 2008), we next measured the clonogenic survival of Mms22L-depleted HeLa cells exposed to topoisomerase I (TopoI) poison camptothecin (CPT). As CPT-induced DSBs at replication forks are mainly repaired by HR-mediated mechanisms, depletion of the HR-promoting gene CtIP was included as a control (Sartori *et al*, 2007). Mms22L was required to protect HeLa cells from CPT treatment, although to a lesser extent than CtIP (Figure 3H). Together, we conclude that Mms22L identifies an evolutionarily conserved pathway required to repair DNA damage during S phase, possibly by promoting replication-associated HR.

Mms22L is degraded upon DNA damage induced during S phase

To characterise the Mms22L protein, we raised polyclonal antibodies against the N-terminal 325 amino acid fragment of Mms22L. Immunoblot analysis detected a single band of ~130 kDa, which was strongly reduced upon depletion of Mms22L by RNAi (Figure 3A). To examine cell cycle expression of endogenous Mms22L, we synchronised HeLa cells in early S phase using a double thymidine block/release (DTB/R) protocol (Sumara *et al*, 2007). Mms22L was expressed throughout S and G2 phase, but its levels were reduced upon entering G1 (Figure 4A), indicating that Mms22L may be regulated in a cell cycle-dependent manner.

To examine the subcellular localisation of Mms22L, we first analysed the localisation of an HA-2xStrep (HSS)-tagged version of Mms22L in transiently transfected HeLa cells. As shown in Figure 4B, HSS-Mms22L was primarily nuclear, and this localisation did not change during the cell cycle or after treatment of cells with CPT (data not shown). Consistent with these results, biochemical fractionation revealed that endogenous Mms22L was enriched in the chromatin fraction, but was solubilised by DNA digestion and high-salt treatment (Figure 4C). Together, these results suggest that a fraction of Mms22L is associated with chromosomes to support genome stability during S phase.

We observed that the levels of HSS-Mms22L strongly increased in cells RNAi-depleted for Cul4A/B or Ddb1 (Figure 4D), suggesting that Mms22L is an unstable protein that is degraded in a Cul4-dependent manner. Therefore, we

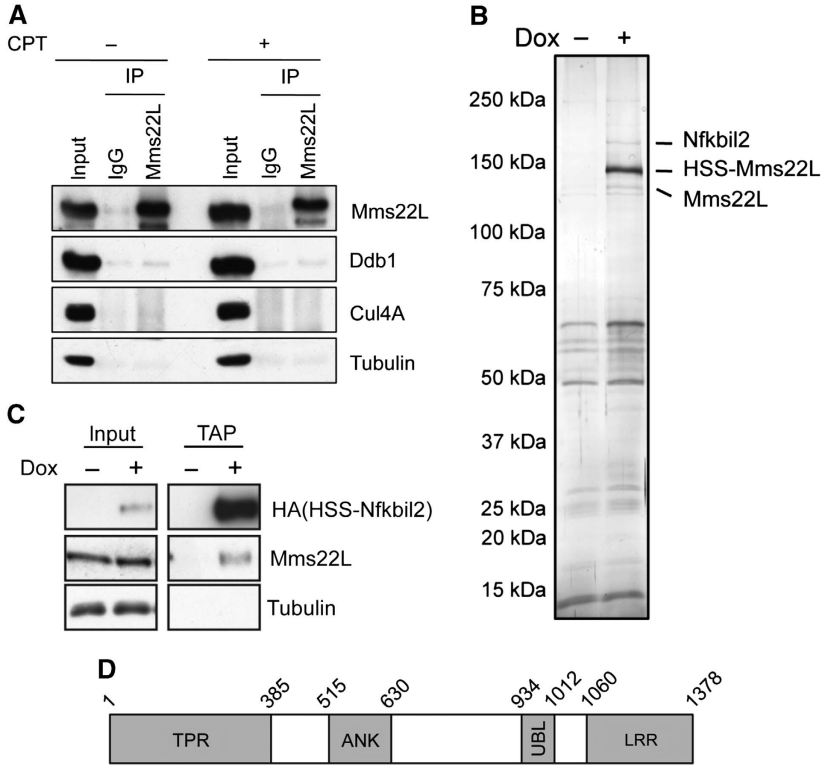

Figure 5 Mms22L stably interacts with the scaffold-like protein Nfkbil2. (**A**) Cul4 and Ddb1 do not co-immunoprecipitate with Mms22L. HeLa cells were treated (+) or not treated (−) with 1 μM CPT for 1 h. Total extracts (input) were immunoprecipitated (IP) with unspecific control IgG (IgG) or anti-Mms22L antibodies, and the presence of Cul4A and Ddb1 was analysed by immunoblotting. (**B**, **C**) HSS-Mms22L co-purifies with endogenous Nfkbil2. HeLa cells stably expressing HSS-Mms22L (**B**) or HSS-Nfkbil2 (**C**) from a doxycycline-inducible promoter were treated for 24 h with (+) or without (−) doxycycline (Dox). The tagged proteins were TAP purified from extracts and associated proteins visualised by silver staining after SDS–PAGE (**B**) or immunoblotting with the indicated antibodies (**C**). The indicated proteins in panel B were identified by mass spectrometry. (**D**) Schematic representation of the domain architecture of Nfkbil2. The following domains were identified; TPR—tetratricopeptide repeat domain, ANK—ankyrin repeat domain, UBL—ubiquitin-like fold, LRR—leucine-rich repeat domain.

tested the stability of endogenous Mms22L in asynchronous and S phase-arrested HeLa cells by CHX chase and found that Mms22L was stable under these conditions (Supplementary Figure 5 and data not shown). However, Mms22L levels were specifically reduced in S phase cells exposed to CPT, and the half-life of Mms22L decreased to ~2 h (Figure 4E and Supplementary Figure 5). A similar reduction was also observed after treating S phase cells with the DNA-methylating agent methyl methanesulphonate (MMS), but not hydroxyurea (HU), which stalls replication forks without inducing DSBs (Figure 4F). Although we were unable to detect ubiquitylated forms of Mms22L, its degradation was dependent on the activity of the ubiquitin-proteasome system (UPS) and DNA damage checkpoint signalling, as it was blocked by addition of the proteasome inhibitor MG132 and caffeine, respectively (Figure 4F and Supplementary Figure 5). Taken together, these results suggest that Mms22L activity upon replication stress is regulated by a Cul4- and ATM/ATR-dependent mechanism.

Mms22L stably interacts with Nfkbil2

Prompted by the homology to yeast Mms22, we first examined whether Mms22L may stably interact with Cul4 and its linker Ddb1. However, we were unable to detect Cul4A or Ddb1 in Mms22L immunoprecipitates, even when the cells were treated with CPT to induce DNA damage (Figure 5A). Similar results were also obtained by immunoprecipitating endogenous Cul4A or FLAG-tagged Mms22L overexpressed in HeLa or U2OS cells after transient transfection (Supplementary Figure 6). Thus, we conclude that, in contrast to yeast, human Mms22L does not stably interact with Cul4 complexes.

To find Mms22L interaction partners, we created a HeLa cell line stably expressing HSS-Mms22L from the tetracycline (Dox)-inducible promoter, and purified associated proteins by tandem-affinity purification (TAP) using streptavidin, followed by anti-HA beads. Eluted proteins were subjected to SDS–PAGE and visualised by silver staining (Figure 5B). In addition to a strong band at the expected molecular weight of HSS-Mms22L, we observed two specific interactors, which we identified by mass spectrometry, as Mms22L and Nfkbil2 (nuclear factor of kappa light polypeptide gene enhancer in B-cells inhibitor-like 2) (Ray *et al*, 1995). To confirm the Mms22L–Nfkbil2 interaction, we constructed an HSS-tagged version of Nfkbil2 under control of the tetracycline-inducible promoter and stably integrated this construct in HeLa cells. Indeed, TAP purifications demonstrated that endogenous Mms22L was detected in induced but not in non-induced control samples (Figure 5C), demonstrating that these proteins form a stable complex *in vivo*. Bioinformatic analysis of the Nfkbil2 protein revealed several well-defined protein–protein interaction domains including TPR and ANK repeats, as well as an LRR domain at its C-terminus (Figure 5D). Moreover, we detected a

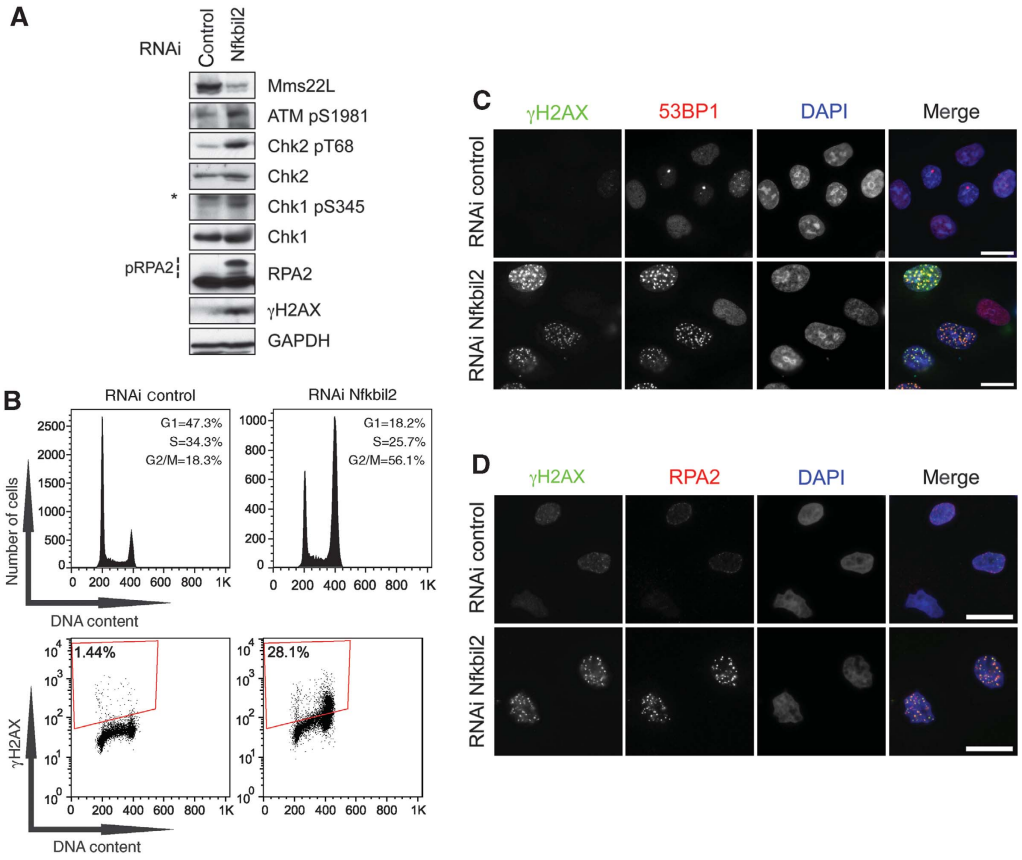

Figure 6 Nfkbil2 is functionally linked to Mms22L. (**A**) Extracts from HeLa cells treated with control or Nfkbil2 (oligo 2) siRNAs for 3 days were analysed by immunoblotting with the indicated antibodies. pRPA2 marks phosphorylated forms of RPA2, while GAPDH controls for equal loading. Nfkbil2 RNAi was confirmed by quantitative RT–PCR (Supplementary Figure 8). Note that Nfkbil2 downregulation leads to reduced levels of Mms22L. The asterisk denotes a cross-reactive band. (**B**) HeLa cells were treated with control or Nfkbil2 (oligo 2) siRNAs for 3 days, and the DNA content and accumulation of DSBs were quantified by flow cytometry after staining with propidium iodide and γH2AX antibodies. The average percentage of γH2AX-positive cells is indicated in the gated area. This experiment was performed in parallel with the one described in 3E, and therefore the same control sample is shown for comparison. (**C**, **D**) HeLa cells were treated with Nfkbil2 (oligo 2) or control siRNAs for 3 days and immunostained with anti-γH2AX, 53BP1 (**C**) and RPA2 (**D**) antibodies. DNA was visualised with DAPI. Scale bar: 20 μm.

conserved stretch with an unique ubiquitin-like (UBL) fold (Supplementary Figure 7). Together, these results demonstrate that Mms22L associates with Nfkbil2, which may function as a scaffolding unit to bridge to multiple protein complexes.

Nfkbil2 is required to maintain genomic stability during S phase

To investigate the functional importance of Nfkbil2, we RNAi-depleted Nfkbil2 from HeLa cells and monitored activation of the DNA damage checkpoint by immunoblot analysis using phospho-specific antibodies against activated checkpoint proteins. Similar to Mms22L, Nfkbil2 depletion resulted in activation of ATM, Chk2 and Chk1, which was accompanied by hyperphosphorylation of RPA2 and γH2AX (Figure 6A and Supplementary Figure 8). Moreover, flow cytometry and indirect immunofluorescence microscopy revealed a strong delay of these cells at the G2/M boundary, which was accompanied by an accumulation of γH2AX foci (Figure 6B, C and D). These γH2AX foci stained positive for 53BP1 and RPA2 (Figure 6C and D, Supplementary Figure 8), implying that cells require Nfkbil2 function to prevent the formation of DSBs during DNA replication. Interestingly, Mms22L levels were strongly decreased in the absence of Nfkbil2 (Figure 6A), indicating that binding of Nfkbil2 stabilises Mms22L *in vivo*. Taken together, these data suggest that Mms22L and Nfkbil2 may function together to maintain genome integrity during DNA replication.

Nfkbil2 links Mms22L function to components involved in DNA replication and repair

To better understand the function of the Mms22L–Nfkbil2 complex, we TAP-purified HSS-Nfkbil2 expressed from the tetracycline-inducible promoter in HeLa cells treated with or without CPT. In addition to Mms22L, silver-stained Nfkbil2 preparations separated by SDS–PAGE revealed multiple interacting proteins (Figure 7A). Mass spectrometry analysis identified several components involved in the regulation of DNA repair and replication, including two subunits of the Ku complex (Ku70/XRCC6 and Ku80/XRCC5), subunits of the replicative helicase (MCM2, 4 and 6), the histone chaperones Asf1A, Asf1B and FACT, as well as histones H1, H2A and H2B (Figure 7B and Supplementary Table 4). Interestingly, some proteins such as Asf1B and the subunits of the FACT complex Spt16 and Ssrp1 were only detected in samples treated with CPT. Immunoblotting with specific antibodies confirmed the

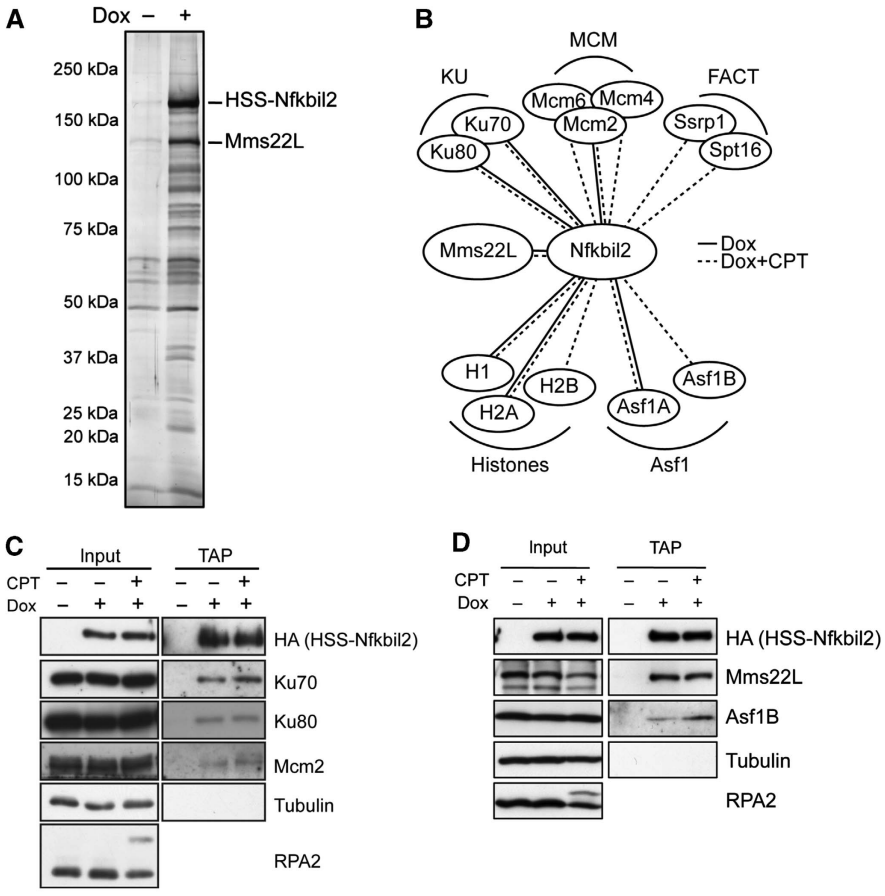

Figure 7 Nfkbil2 links Mms22L function to components involved in DNA replication and repair. TAP purifications from HeLa cells stably expressing HSS-Nfkbil2 induced (+) or not induced (−) with doxycycline (Dox) were visualised by silver staining (**A**). The positions of HSS-Nfkbil2 and endogenous Mms22L are indicated. Where indicated, cells were treated with 1 μM CPT for the last hour before harvesting (+ CPT). Purified proteins were identified by mass spectrometry (**B**, and Supplementary Table 2), and confirmed by immunoblotting with specific antibodies (**C**, **D**).

presence of Ku70 and Ku80 in HSS-Nfkbil2 purifications (Figure 7C) and their abundance was not significantly altered in the presence of CPT. In contrast, binding of Nfkbil2 to Mcm2 and Asf1B was slightly increased under these conditions (Figure 7C and D), indicating that some interactions with Nfkbil2 may indeed be regulated by DNA replication stress. Together, these findings suggest that Nfkbil2 and Mms22L are stably associated core components of a larger repair complex, which may be recruited to stalled replication forks to prevent the formation of DSBs.

Discussion

While the mechanisms and underlying machinery required to duplicate bulk genomic DNA are beginning to emerge, much less is known about how cells replicate through damaged templates or special chromosomal regions. In budding yeast, the Cul4-related Rtt101^{Mms22} complex is required for replication restart after fork collapse and cells accumulate many unreplicated gaps in the absence of this E3 ligase. By RNAi screening and automated phenotypic analysis of live-cell movies from HeLa cells expressing cell cycle markers H2B-mCherry and EGFP-PCNA, we have identified several human Cul4-associated proteins, which are required for faithful progression through G1 and S phase. We also identified and characterised two novel components, Mms22L and its interaction partner Nfkbil2, which function in a conserved pathway required to protect replication forks from collapse during normal S phase.

Multiple Cul4-based complexes regulate progression through G1 and S phase

Cul4 has been implicated in the regulation of cell cycle progression and various DNA transactions and chromatin remodelling (Higa and Zhang, 2007). More than 50 associated DCAFs have been identified, which interact via Ddb1 and are thought to serve as substrate-specific adaptors in Cul4-based ligase complexes (Lee and Zhou, 2007). Several DCAFs have previously been implicated in processes related to DNA replication and repair. For example, Cdt2 regulates degradation of the licensing factor Cdt1, and thereby prevents DNA re-replication (Jin *et al*, 2006). Cdt2 also triggers degradation of the translesion polymerase Polη upon DNA damage in *Caenorhabditis elegans* (Kim and Michael, 2008). Using a high-content RNAi-screening approach, we identified several *bona fide* DCAFs and Cul4-associated proteins inducing significant G1 delays. Among them, the two DCAFs EED and Wdr5 regulate histone methylation and interact with endogenous Cul4B (Higa *et al*, 2006). Likewise, downregulation of the putative oncoprotein WDSOF1 (Chin *et al*, 2007) and Tbl3

associated with polycystic kidney disease (Weinstat-Saslow *et al*, 1993) results in a strong G1 delay (Supplementary Table 2), but their precise functions remain to be explored. Two genes required for G1 progression, *Wdr12* and *Pwp2*, have been linked to ribosome biogenesis (Dosil and Bustelo, 2004; Rohrmoser *et al*, 2007). Wdr12 binds to the nucleolar proteins Bop1 and Pes1, while Pwp2 associates with 35S pre-rRNA, suggesting that the $Cul4^{Wdr12}$ and $Cul4^{Pwp2}$ complexes may ubiquitylate substrates involved in rRNA processing. Interestingly, only seven Cul4-linked genes including four *bona fide* DCAFs exhibit a specific S phase delay with no significant prolongation of G1 or G2. While the underlying defects and molecular mechanisms remain to be investigated, our results demonstrate that distinct Cul4-based E3 ligases regulate multiple processes during G1 and S phase, and provide an important step towards identifying biologically relevant substrates. In addition to *bona fide* DCAFs, we also examined the function of a large set of Cul4-interacting proteins for cell cycle progression. Although it is not clear how these binding partners affect Cul4 activity, our phenotypic analysis may help to link them to specific Cul4-dependent processes.

C6orf167/Mms22L is homologous to yeast Mms22, but may not function as a substrate adaptor in a Cul4 complex

We found that C6orf167/Mms22L exhibits significant sequence and functional similarities to yeast Mms22. Although the overall sequence homology is low and mainly confined to few stretches, evolutionary analysis revealed that many eukaryotic species encode at least one Mms22L (Supplementary Figure 1). In budding yeast, Mms22 supports progression of replication through natural pause sites and damaged DNA in a complex with Rtt101 and Mms1, homologues of human Cul4 and Ddb1 proteins, respectively (Zaidi *et al*, 2008). Yeast Mms22 also binds several replication fork-associated proteins, including Ctf4 and Rtt107, suggesting that it functions at stalled replication forks to promote fork repair and restart functions (Mimura *et al*, 2010). On the basis of interaction studies, we previously proposed that Mms22 might function as a substrate adaptor in the Rtt101/Cul4-based complex, which recognises and ubiquitylates proteins specifically at stalled replication forks. Interestingly, Mms22 is itself ubiquitylated and degraded in an Rtt101-dependent manner (Ben-Aroya *et al*, 2010), suggesting that Mms22 may also be a substrate of the Rtt101 complex. We were unable to detect a stable interaction between Mms22L and Cul4/Ddb1 in HeLa cells, but Mms22L stability was dependent on the presence of Cul4 and Ddb1. In addition, Mms22L was rapidly degraded in S phase cells exposed to DNA-damaging agents inducing DSBs such as CPT and MMS and this instability required the activity of the ATM/ATR checkpoint kinases. Although the function of this damage-induced degradation of Mms22L during S phase is not clear at present, it is tempting to speculate that it is linked to the Mms22L-mediated repair process; for example, removing the repair complex from the DNA template to resume DNA replication.

Mms22L stably interacts with Nfkbil2 to prevent replication fork collapse during S phase

Several lines of evidence suggest that Mms22L and Nfkbil2 function together regulating the integrity of stalled replication forks. First, Mms22L and Nfkbil2 form a stable complex and Mms22L levels are strongly reduced in the absence of Nfkbil2. Second, downregulation of either protein results in specific replication defects leading to a pronounced G2 delay caused by activation of the ATM/ATR checkpoint. Nfkbil2 has previously been implicated in the regulation of NFκB signalling based on its partial homology to inhibitors of NFκB (IκBs) (Ray *et al*, 1995). However, our results strongly suggest that the Mms22L–Nfkbil2 complex is involved in promoting replication fork progression during S phase, most likely by preventing replication fork collapse upon replication stress. Indeed, Mms22L- or Nfkbil2-depleted cells accumulate spontaneous DSBs accompanied by extended ssDNA stretches that may result from increased DNA end resection, a prerequisite for HR-mediated repair. These defects are reminiscent of yeast Mms22, which is required for HR-mediated repair upon replisome stalling, but is not necessary for HR repair of DSBs (Duro *et al*, 2008). Thus, we speculate that, analogous to yeast Mms22, the Mms22L–Nfkbil2 complex may be involved in the recognition and resolution of HR intermediates formed at replication forks stalled at sites that are particularly difficult to replicate, such as replication slow zones or fragile sites.

Interestingly, Nfkbil2 is characterised by the presence of three well-defined protein–protein interaction domains (seven tetratricopeptide repeats in the N-terminus, three central ankyrin repeats and six C-terminal leucine-rich repeats), and a unique type of ubiquitin-like fold (Supplementary Figure 7). Although Nfkbil2 has no obvious homologues in budding yeast, a similar UBL fold is present in Tof2, Net1 and possibly Esc2. All these proteins interact with the histone deacetylase Sir2 and are thought to prevent excessive HR at replication slow zones, in particular at telomeres and rDNA loci (Cuperus and Shore, 2002; Huang *et al*, 2006; Mankouri *et al*, 2009). Esc2 was recently reported to directly interact with the Rtt101–Mms1 complex (Mimura *et al*, 2010), suggesting an intriguing link to replication fork repair mechanisms.

The Mms22L–Nfkbil2 complex may function as a scaffold to assemble the replication fork repair machinery

Consistent with its scaffold-like domain composition, Nfkbil2 interacts with histones H1, H2A and H2B, and with several known chromatin remodelling and DNA replication/repair factors. The association with a subset of these components was slightly enhanced upon replication stress, indicating regulated recruitment to stalled replication forks. Asf1A/B and FACT are evolutionarily conserved histone deposition complexes that alter chromatin composition and thereby facilitate progression of DNA replication forks and enable efficient DNA repair (Ransom *et al*, 2010). The FACT complex promotes binding of DNA repair factors by replacing γH2AX at damaged sites with the canonical H2A variant (Heo *et al*, 2008) and is antagonised by the poly ADP ribose polymerase, PARP1, an enzyme modulating the choice between the NHEJ and HR repair pathways at stalled forks (Saberi *et al*, 2007). Thus, it is possible that the interaction of FACT with the Mms22L–Nfkbil2 complex may influence which DNA repair pathway is used at stalled forks. Consistent with this notion, yeast Mms22 promotes sister chromatid exchange induced by replisome stalling (Duro *et al*, 2008), possibly by regulating

Rtt101-dependent ubiquitylation of the FACT subunit Spt16 (Han *et al*, 2010). Moreover, Rtt101 is recruited to chromatin by a mechanism that requires the H3-K56 acetyltransferase Rtt109 and the histone chaperone Asf1 (Collins *et al*, 2007; Roberts *et al*, 2008). Human Asf1 has also been linked to H3-K56 acetylation, and this pathway is involved in recovery from replication stress (Yuan *et al*, 2009). Thus, it is tempting to speculate that the Mms22L–Nfkbil2 complex, together with FACT and Asf1, may influence repair pathways by regulating the chromatin state at stalled replication forks.

Surprisingly, we found that Nfkbil2 associates with Ku70 and Ku80, two proteins involved in NHEJ repair. Ku heterodimers bind with high affinity to DSBs and recruit DNA-PK and Ligase4-XRCC4 to ligate the termini without or with minimal homology. Although NHEJ operates preferentially during G1, both NHEJ and HR pathways have been implicated in repair of replication-dependent DNA damage in human cells (Arnaudeau *et al*, 2001; Lundin *et al*, 2002). Consistent with this notion, both Ku proteins are abundant nuclear proteins (Downs and Jackson, 2004), and DNA-PK is activated by DSBs occurring specifically during S phase (Chen *et al*, 2005). Thus, the HR and NHEJ machineries may cooperate in processing DSBs during S phase and the Mms22L–Nfkbil2 complex may interact with the Ku heterodimer to regulate specific types of repair at stalled forks. Ku proteins might also work independently of the catalytic components of NHEJ to cap DSB ends at collapsed forks and thereby prevent their promiscuous resection. Further studies are now required to demonstrate the functional importance of the interaction of Ku proteins with the Nfkbil2–Mms22L complex during replication stress.

Materials and methods

Cell culture

HeLa and U2OS cells were cultured in Dulbecco's modified Eagle's medium (DMEM) supplemented with 10% fetal bovine serum (FBS, PAA), 0.2 mM L-glutamine and standard antibiotics. Thymidine block and release experiments (DTB/R) were performed as described previously (Sumara *et al*, 2007). The FRT-TetR-HeLa cell line for creating stable cell lines using the Flp-In System (Invitrogen) was kindly provided by S Taylor (University of Manchester), and maintained as described (Tighe *et al*, 2008). The HSS-tagged Mms22L and Nfkbil2 cell lines were generated as described (Glatter *et al*, 2009). HeLa cells stably co-expressing H2B-mCherry and EGFP-PCNA were cultured in DMEM with 10% FBS containing 0.5 mg/ml G418 and 0.5 μg/ml puromycin (Held *et al*, 2010). For overexpression, DNA plasmid transfections were performed with Lipofectamine 2000 (Invitrogen) or JetPEI (PolyPlus) following the manufacturer's instructions. For RNAi experiments, HeLa or U2OS cells were transfected with 50 nM siRNAs using Lipofectamine RNAiMAX (Invitrogen) for 48 or 72 h. Downregulation of the targets was confirmed by immunoblotting with specific antibodies or quantitative RT–PCR. The sequences of all siRNA oligos used in this study are listed in Supplementary data.

For clonogenic survival assays, HeLa cells were split 2 days after RNAi and seeded into six-well dishes in triplicate (500 cells/well). After 24 h, 1 μM CPT was added for 1 h, washed 3 × with DMEM and incubated for 8–10 days. Colonies were counted after staining cells with 0.25% crystal violet in 80% methanol.

RNAi screening using automated live-cell microscopy

The siRNA oligos used in the screen are listed in Supplementary Table 2. RNAi screening was performed as described (Schmitz *et al*, 2010), with minor adjustments. Briefly, siRNA duplexes (20 nM final concentration) from Qiagen were reverse transfected with RNAiMAX (Invitrogen) in 96-well microscopy plates (μClear, Greiner). After 21 h, cells were washed three times with full media containing phenol red- and riboflavin-free DMEM (Invitrogen) and maintained therein. Automated microscopy was started 25 h after RNAi and continued for 47 h in an incubation chamber on a MD ImageXpress Micro screening microscope equipped with a 10 × 0.5 N.A. S Fluor dry objective (Nikon), controlled by Metamorph. Image analysis was performed using CellCognition software (Held *et al*, 2010). Briefly, cell nuclei and mitotic chromosome masses were detected in the RFP channel, and texture and shape features were calculated for each of these objects in the RFP- and GFP channels. Examples for each class were manually annotated for supervised classification, and the trained classifier then applied for the whole data set. Cells were tracked over time and mitotic events were detected on the basis of the transition from pro- to prometaphase, pro- to metaphase or prometaphase to metaphase. For analysing G1 and S phase, trajectories of ~19 h after mitosis were extracted; for G2 phase, trajectories of around 17 h before mitosis were used. After hidden Markov model-based error correction with a completely free transition model, the duration of the individual cell cycle phases for each cell was measured on the basis of the time between entry into and exit from the specific phase. For scoring hits, the median and the median average deviation for all negative controls were measured and a *z*-score was calculated for each siRNA on the basis of at least 15 independent measurements (Boutros *et al*, 2006).

Immunofluorescence microscopy, flow cytometry and DNA combing

Cultured cells grown on coverslips were fixed either with 4% paraformaldehyde (PFA, in PBS) for 10 min at room temperature (anti-RPA2 staining) or with methanol for 20 min at −20°C (anti-53BP1 and anti-HA stainings). For anti-RPA2 staining, cells were permeabilised for 5 min with 300 mM sucrose, 3 mM $MgCl_2$, 1 mM EDTA, 50 mM NaCl, 25 mM HEPES (pH 7.5), 0.5% Triton X-100 before PFA fixation. Samples were incubated for 1 h with antibodies diluted in PBS containing 0.01% Triton X-100 and 5% FBS. Secondary antibodies were labelled with Alexa fluor 488 or 568 (Invitrogen). Next, 1 μg/ml DAPI was added to visualise DNA. Samples were mounted using Immu-Mount (Thermo) and images were captured on a Leica DM6000B epifluorescence microscope.

For flow cytometry, cells were stained for DNA and γH2AX levels, as described previously (Olma *et al*, 2009). Samples were analysed with a FACSCalibur flow cytometer (BD Biosciences) using CellQuest and FlowJo software. DNA combing was performed as described previously (Tuduri *et al*, 2009), with minor modifications as described in Supplementary data.

Extract preparation and chromatin fractionation

Extracts from cultured cells were prepared in extraction buffer (20 mM Tris–HCl (pH 7.5), 150 mM NaCl, 0.2% Nonidet P-40, 20 mM β-glycerophosphate, 10% glycerol, 1 mM NaF, 0.5 mM DTT and complete protease inhibitor cocktail; Roche) by passing the cell suspension through a 27G needle. For chromatin fractionation, 2×10^8 cells were suspended in 1 ml hypotonic buffer (10 mM Tris–HCl (pH 7.5), 10 mM KCl, 1.5 mM $MgCl_2$, 10 mM β-mercaptoethanol and 0.2 mM PMSF) and disrupted by Dounce homogenisation. Cytosol and nuclei were separated by centrifugation at 2000 *g* for 15 min at 4°C. Nuclei were resuspended in 1 ml extraction buffer (15 mM Tris–HCl (pH 7.5), 400 mM NaCl, 1 mM $MgCl_2$, 10% glycerol, 1 mM EDTA, 10 mM β-mercaptoethanol and 0.2 mM PMSF). After incubating on ice for 30 min, the samples were centrifuged at 20 000 *g* for 30 min at 4°C and the supernatants were used as nuclear fraction. The chromatin pellet was washed and resuspended in digestion buffer (20 mM Tris–HCl (pH 7.5), 100 mM KCl, 2 mM $MgCl_2$, 1 mM $CaCl_2$, 0.3 M sucrose, 0.1% Triton X-100 and complete protease inhibitor cocktail; Roche), and incubated for 1 h at 4°C with 2 U/ml of micrococcal nuclease. The reaction was terminated with 5 mM EGTA/EDTA, and the KCl concentration was adjusted to 300 mM in one-half of the sample. After 1 h at 4°C, the samples were centrifuged for 10 min at 8000 *g* and the supernatant used as solubilised chromatin fraction.

DNA and RNA manipulations, immunoblotting and immunoprecipitation experiments

Standard protocols were used for DNA and RNA manipulations as described in Supplementary data. For immunoblotting, proteins were resolved by SDS–PAGE and transferred to PVDF immobilon-P membrane (Millipore). Blocking and antibody incubations were carried out in 5% low-fat milk (Migros) in TBS-T (150 mM NaCl,

20 mM Tris (pH 8.0) and 0.1% Tween-20), and washings in TBS-T. Blots were developed using Immun-Star™ HRP (Biorad). For immunoprecipitation experiments, 1 μg of affinity-purified antibodies per 200 μg extracts was incubated for 1 h at 4°C and precipitated using Affiprep protein A beads (Biorad) for 1 h at 4°C. The beads were washed four times with extraction buffer, bound proteins eluted with sample buffer at 95°C and analysed by immunoblotting. All antibodies used in this study are described in Supplementary data.

TAP purifications and mass spectrometry analysis

TAP purifications were essentially carried out as described (Wyler *et al*, 2010). Briefly, expression of the bait protein in HeLa cells was induced by 1 μg/ml doxycyclin 24 h before harvesting by scratching. Cells were lysed using 27G needles in TAP buffer (10 mM Tris (pH 7.5), 100 mM KCl, 2 mM MgCl2, 0.5% NP40, 300 mM sucrose, 10 mM β-glycerophosphate, 0.2 mM Na_3VO_4, 1 mM ATP and complete protease inhibitors; Roche) containing 0.5 mM DTT. Extracts were cleared by centrifugation for 15 min at 5400 *g* and incubated with pre-equilibrated StrepTactin beads (IBA, 50 μl per 15 cm dish) for 30 min on an overhead shaker. Beads were washed four times with TAP buffer and proteins eluted with 3 × 300 μl TAP buffer containing 10 mM Biotin (Sigma). Eluates were incubated with pre-equilibrated anti-HA beads (Sigma; 12.5 μl beads per 15 cm dish) for 1 h. For analysis on SDS–PAGE, beads were washed four times with TAP buffer, once with TAP buffer without KCl and eluted with Laemmli buffer without DTT. After elution, DTT was added to 20 mM final concentration. Mass spectrometry analysis was performed as described in Supplementary data.

Supplementary data

Supplementary data are available at *The EMBO Journal* Online (http://www.embojournal.org).

Acknowledgements

We thank D Durocher, W Harper and J Rouse for communicating unpublished results; S Taylor, M Gstaiger, U Kutay and E Wyler for providing cell lines and plasmids; T Roberts for critical reading of the manuscript; and members of the Peter lab for helpful discussions. We are indebted to G Csucs and N Graf for advice on imaging issues and data storage, and the D-BIOL RNAi screening facility LMC/RISC. This work was supported by Oncosuisse, the Swiss National Science Foundation (SNF) and the ETH Zürich. The work was supported in part by a grant from the Scottish Government to the Scottish Institute for Cell Signaling.

Conflict of interest

The authors declare that they have no conflict of interest.

References

Abbas T, Sivaprasad U, Terai K, Amador V, Pagano M, Dutta A (2008) PCNA-dependent regulation of p21 ubiquitylation and degradation via the CRL4Cdt2 ubiquitin ligase complex. *Genes Dev* **22:** 2496–2506

Anantha RW, Vassin VM, Borowiec JA (2007) Sequential and synergistic modification of human RPA stimulates chromosomal DNA repair. *J Biol Chem* **282:** 35910–35923

Arnaudeau C, Lundin C, Helleday T (2001) DNA double-strand breaks associated with replication forks are predominantly repaired by homologous recombination involving an exchange mechanism in mammalian cells. *J Mol Biol* **307:** 1235–1245

Ben-Aroya S, Agmon N, Yuen K, Kwok T, McManus K, Kupiec M, Hieter P (2010) Proteasome nuclear activity affects chromosome stability by controlling the turnover of Mms22, a protein important for DNA repair. *PLoS Genet* **6:** e1000852

Binz SK, Sheehan AM, Wold MS (2004) Replication protein A phosphorylation and the cellular response to DNA damage. *DNA Repair (Amst)* **3:** 1015–1024

Boutros M, Bras LP, Huber W (2006) Analysis of cell-based RNAi screens. *Genome Biol* **7:** R66

Branzei D, Foiani M (2008) Regulation of DNA repair throughout the cell cycle. *Nat Rev Mol Cell Biol* **9:** 297–308

Chen BP, Chan DW, Kobayashi J, Burma S, Asaithamby A, Morotomi-Yano K, Botvinick E, Qin J, Chen DJ (2005) Cell cycle dependence of DNA-dependent protein kinase phosphorylation in response to DNA double strand breaks. *J Biol Chem* **280:** 14709–14715

Chin SF, Teschendorff AE, Marioni JC, Wang Y, Barbosa-Morais NL, Thorne NP, Costa JL, Pinder SE, van de Wiel MA, Green AR, Ellis IO, Porter PL, Tavare S, Brenton JD, Ylstra B, Caldas C (2007) High-resolution aCGH and expression profiling identifies a novel genomic subtype of ER negative breast cancer. *Genome Biol* **8:** R215

Cimprich KA, Cortez D (2008) ATR: an essential regulator of genome integrity. *Nat Rev Mol Cell Biol* **9:** 616–627

Collins SR, Miller KM, Maas NL, Roguev A, Fillingham J, Chu CS, Schuldiner M, Gebbia M, Recht J, Shales M, Ding H, Xu H, Han J, Ingvarsdottir K, Cheng B, Andrews B, Boone C, Berger SL, Hieter P, Zhang Z *et al* (2007) Functional dissection of protein complexes involved in yeast chromosome biology using a genetic interaction map. *Nature* **446:** 806–810

Cortez D (2003) Caffeine inhibits checkpoint responses without inhibiting the ataxia-telangiectasia-mutated (ATM) and ATM- and Rad3-related (ATR) protein kinases. *J Biol Chem* **278:** 37139–37145

Cuperus G, Shore D (2002) Restoration of silencing in Saccharomyces cerevisiae by tethering of a novel Sir2-interacting protein, Esc8. *Genetics* **162:** 633–645

Dosil M, Bustelo XR (2004) Functional characterization of Pwp2, a WD family protein essential for the assembly of the 90 S pre-ribosomal particle. *J Biol Chem* **279:** 37385–37397

Downs JA, Jackson SP (2004) A means to a DNA end: the many roles of Ku. *Nat Rev Mol Cell Biol* **5:** 367–378

Duro E, Vaisica JA, Brown GW, Rouse J (2008) Budding yeast Mms22 and Mms1 regulate homologous recombination induced by replisome blockage. *DNA Repair (Amst)* **7:** 811–818

Fousteri M, Vermeulen W, van Zeeland AA, Mullenders LH (2006) Cockayne syndrome A and B proteins differentially regulate recruitment of chromatin remodeling and repair factors to stalled RNA polymerase II *in vivo*. *Mol Cell* **23:** 471–482

Glatter T, Wepf A, Aebersold R, Gstaiger M (2009) An integrated workflow for charting the human interaction proteome: insights into the PP2A system. *Mol Syst Biol* **5:** 237

Han J, Li Q, McCullough L, Kettelkamp C, Formosa T, Zhang Z (2010) Ubiquitylation of FACT by the cullin-E3 ligase Rtt101 connects FACT to DNA replication. *Genes Dev* **24:** 1485–1490

Held M, Schmitz MH, Fischer B, Walter T, Neumann B, Olma MH, Peter M, Ellenberg J, Gerlich DW (2010) CellCognition: time-resolved phenotype annotation in high-throughput live cell imaging. *Nat Methods* **7:** 747–754

Heo K, Kim H, Choi SH, Choi J, Kim K, Gu J, Lieber MR, Yang AS, An W (2008) FACT-mediated exchange of histone variant H2AX regulated by phosphorylation of H2AX and ADP-ribosylation of Spt16. *Mol Cell* **30:** 86–97

Higa LA, Wu M, Ye T, Kobayashi R, Sun H, Zhang H (2006) CUL4-DDB1 ubiquitin ligase interacts with multiple WD40-repeat proteins and regulates histone methylation. *Nat Cell Biol* **8:** 1277–1283

Higa LA, Zhang H (2007) Stealing the spotlight: CUL4-DDB1 ubiquitin ligase docks WD40-repeat proteins to destroy. *Cell Div* **2:** 5

Huang J, Brito IL, Villen J, Gygi SP, Amon A, Moazed D (2006) Inhibition of homologous recombination by a cohesin-associated clamp complex recruited to the rDNA recombination enhancer. *Genes Dev* **20:** 2887–2901

Jin J, Arias EE, Chen J, Harper JW, Walter JC (2006) A family of diverse Cul4-Ddb1-interacting proteins includes Cdt2, which is required for S phase destruction of the replication factor Cdt1. *Mol Cell* **23:** 709–721

Kapetanaki MG, Guerrero-Santoro J, Bisi DC, Hsieh CL, Rapic-Otrin V, Levine AS (2006) The DDB1-CUL4ADDB2 ubiquitin ligase is deficient in xeroderma pigmentosum group E and targets histone H2A at UV-damaged DNA sites. *Proc Natl Acad Sci USA* **103:** 2588–2593

Kim SH, Michael WM (2008) Regulated proteolysis of DNA polymerase eta during the DNA-damage response in C. elegans. *Mol Cell* **32:** 757–766

Kim Y, Kipreos ET (2007) Cdt1 degradation to prevent DNA re-replication: conserved and non-conserved pathways. *Cell Div* **2:** 18

Lee J, Zhou P (2007) DCAFs, the missing link of the CUL4-DDB1 ubiquitin ligase. *Mol Cell* **26:** 775–780

Lovejoy CA, Lock K, Yenamandra A, Cortez D (2006) DDB1 maintains genome integrity through regulation of Cdt1. *Mol Cell Biol* **26:** 7977–7990

Luke B, Versini G, Jaquenoud M, Zaidi IW, Kurz T, Pintard L, Pasero P, Peter M (2006) The cullin Rtt101p promotes replication fork progression through damaged DNA and natural pause sites. *Curr Biol* **16:** 786–792

Lundin C, Erixon K, Arnaudeau C, Schultz N, Jenssen D, Meuth M, Helleday T (2002) Different roles for nonhomologous end joining and homologous recombination following replication arrest in mammalian cells. *Mol Cell Biol* **22:** 5869–5878

Mankouri HW, Ngo HP, Hickson ID (2009) Esc2 and Sgs1 act in functionally distinct branches of the homologous recombination repair pathway in Saccharomyces cerevisiae. *Mol Biol Cell* **20:** 1683–1694

Mimura S, Yamaguchi T, Ishii S, Noro E, Katsura T, Obuse C, Kamura T (2010) Cul8/Rtt101 forms a variety of protein complexes that regulate DNA damage response and transcriptional silencing. *J Biol Chem* **285:** 9858–9867

Olma MH, Roy M, Le Bihan T, Sumara I, Maerki S, Larsen B, Quadroni M, Peter M, Tyers M, Pintard L (2009) An interaction network of the mammalian COP9 signalosome identifies Dda1 as a core subunit of multiple Cul4-based E3 ligases. *J Cell Sci* **122:** 1035–1044

Pintard L, Willems A, Peter M (2004) Cullin-based ubiquitin ligases: Cul3-BTB complexes join the family. *Embo J* **23:** 1681–1687

Ransom M, Dennehey BK, Tyler JK (2010) Chaperoning histones during DNA replication and repair. *Cell* **140:** 183–195

Ray P, Zhang DH, Elias JA, Ray A (1995) Cloning of a differentially expressed I kappa B-related protein. *J Biol Chem* **270:** 10680–10685

Roberts TM, Zaidi IW, Vaisica JA, Peter M, Brown GW (2008) Regulation of rtt107 recruitment to stalled DNA replication forks by the cullin rtt101 and the rtt109 acetyltransferase. *Mol Biol Cell* **19:** 171–180

Rohrmoser M, Holzel M, Grimm T, Malamoussi A, Harasim T, Orban M, Pfisterer I, Gruber-Eber A, Kremmer E, Eick D (2007) Interdependence of Pes1, Bop1, and WDR12 controls nucleolar localization and assembly of the PeBoW complex required for maturation of the 60S ribosomal subunit. *Mol Cell Biol* **27:** 3682–3694

Saberi A, Hochegger H, Szuts D, Lan L, Yasui A, Sale JE, Taniguchi Y, Murakawa Y, Zeng W, Yokomori K, Helleday T, Teraoka H, Arakawa H, Buerstedde JM, Takeda S (2007) RAD18 and poly(ADP-ribose) polymerase independently suppress the access of nonhomologous end joining to double-strand breaks and facilitate homologous recombination-mediated repair. *Mol Cell Biol* **27:** 2562–2571

Sartori AA, Lukas C, Coates J, Mistrik M, Fu S, Bartek J, Baer R, Lukas J, Jackson SP (2007) Human CtIP promotes DNA end resection. *Nature* **450:** 509–514

Schmitz MH, Held M, Janssens V, Hutchins JR, Hudecz O, Ivanova E, Goris J, Trinkle-Mulcahy L, Lamond AI, Poser I, Hyman AA, Mechtler K, Peters JM, Gerlich DW (2010) Live-cell imaging RNAi screen identifies PP2A-B55alpha and importin-beta1 as key mitotic exit regulators in human cells. *Nat Cell Biol* **12:** 886–893

Schultz LB, Chehab NH, Malikzay A, Halazonetis TD (2000) p53 binding protein 1 (53BP1) is an early participant in the cellular response to DNA double-strand breaks. *J Cell Biol* **151:** 1381–1390

Shiloh Y (2003) ATM and related protein kinases: safeguarding genome integrity. *Nat Rev Cancer* **3:** 155–168

Sonoda E, Sasaki MS, Buerstedde JM, Bezzubova O, Shinohara A, Ogawa H, Takata M, Yamaguchi-Iwai Y, Takeda S (1998) Rad51-deficient vertebrate cells accumulate chromosomal breaks prior to cell death. *EMBO J* **17:** 598–608

Sugasawa K, Okuda Y, Saijo M, Nishi R, Matsuda N, Chu G, Mori T, Iwai S, Tanaka K, Hanaoka F (2005) UV-induced ubiquitylation of XPC protein mediated by UV-DDB-ubiquitin ligase complex. *Cell* **121:** 387–400

Sumara I, Quadroni M, Frei C, Olma MH, Sumara G, Ricci R, Peter M (2007) A Cul3-based E3 ligase removes Aurora B from mitotic chromosomes, regulating mitotic progression and completion of cytokinesis in human cells. *Dev Cell* **12:** 887–900

Sutterluty H, Chatelain E, Marti A, Wirbelauer C, Senften M, Muller U, Krek W (1999) p45SKP2 promotes p27Kip1 degradation and induces S phase in quiescent cells. *Nat Cell Biol* **1:** 207–214

Tighe A, Staples O, Taylor S (2008) Mps1 kinase activity restrains anaphase during an unperturbed mitosis and targets Mad2 to kinetochores. *J Cell Biol* **181:** 893–901

Tourriere H, Pasero P (2007) Maintenance of fork integrity at damaged DNA and natural pause sites. *DNA Repair (Amst)* **6:** 900–913

Tuduri S, Crabbe L, Conti C, Tourriere H, Holtgreve-Grez H, Jauch A, Pantesco V, De Vos J, Thomas A, Theillet C, Pommier Y, Tazi J, Coquelle A, Pasero P (2009) Topoisomerase I suppresses genomic instability by preventing interference between replication and transcription. *Nat Cell Biol* **11:** 1315–1324

Wang B, Matsuoka S, Carpenter PB, Elledge SJ (2002) 53BP1, a mediator of the DNA damage checkpoint. *Science* **298:** 1435–1438

Wang H, Zhai L, Xu J, Joo HY, Jackson S, Erdjument-Bromage H, Tempst P, Xiong Y, Zhang Y (2006) Histone H3 and H4 ubiquitylation by the CUL4-DDB-ROC1 ubiquitin ligase facilitates cellular response to DNA damage. *Mol Cell* **22:** 383–394

Weinstat-Saslow DL, Germino GG, Somlo S, Reeders ST (1993) A transducin-like gene maps to the autosomal dominant polycystic kidney disease gene region. *Genomics* **18:** 709–711

Wyler E, Zimmermann M, Widmann B, Gstaiger M, Pfannstiel J, Kutay U, Zemp I (2010) Tandem affinity purification combined with inducible shRNA expression as a tool to study the maturation of macromolecular assemblies. *RNA* (doi:10.1261/rna.2325911)

Yuan J, Pu M, Zhang Z, Lou Z (2009) Histone H3-K56 acetylation is important for genomic stability in mammals. *Cell Cycle* **8:** 1747–1753

Zaidi IW, Rabut G, Poveda A, Scheel H, Malmstrom J, Ulrich H, Hofmann K, Pasero P, Peter M, Luke B (2008) Rtt101 and Mms1 in budding yeast form a CUL4(DDB1)-like ubiquitin ligase that promotes replication through damaged DNA. *EMBO Rep* **9:** 1034–1040

